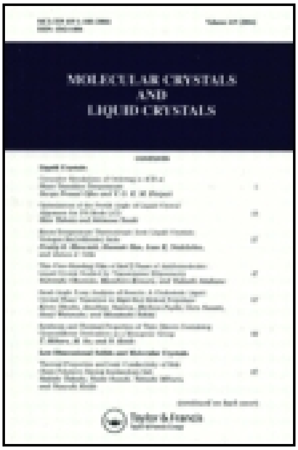

Molecular Crystals and Liquid Crystals Incorporating Nonlinear Optics
Publication details, including instructions for authors and subscription information:
http://www.tandfonline.com/loi/gmcl17

Second Harmonic Generation from Langmuir-Blodgett Films in Various Optical Geometries

K. Kajikawa [a] , K. Kigata [a] , H. Takezoe [a] & A. Fukuda [a]
[a] Tokyo Institute of Technology, Department of Organic and Polymeric Materials, O-okayama, Meguro-ku, Tokyo, 152
Version of record first published: 04 Oct 2006.

To cite this article: K. Kajikawa , K. Kigata , H. Takezoe & A. Fukuda (1990): Second Harmonic Generation from Langmuir-Blodgett Films in Various Optical Geometries, Molecular Crystals and Liquid Crystals Incorporating Nonlinear Optics, 182:1, 91-101

To link to this article: http://dx.doi.org/10.1080/00268949008047791

Mol. Cryst. Liq. Cryst., 1990, Vol. 182A, pp. 91–101
Reprints available directly from the publisher
Photocopying permitted by license only

Printed in the United States of America

Second Harmonic Generation from Langmuir-Blodgett Films in Various Optical Geometries

K. KAJIKAWA, K. KIGATA, H. TAKEZOE and A. FUKUDA

Tokyo Institute of Technology, Department of Organic and Polymeric Materials, O-okayama, Meguro-ku, Tokyo 152

(*Received June 3, 1989; Accepted for publication November 9, 1989; Revised October 21, 1989*)

Second harmonic generation (SHG) from Langmuir-Blodgett films of hemicyanine dye was measured in various optical geometries. It was found that the SH intensities show a great difference in two cases: a) when s-polarized light is incident upon the monolayer from the air side; and b) when it is incident from behind through the glass substrate. In contrast, the difference is negligible for p-polarized light. This fact is true in both transmission and reflection geometries.

Keywords: Second harmonic generation, Langmuir-Blodgett film

I. INTRODUCTION

The Langmuir-Blodgett (LB) technique is expected to serve as a powerful method to construct ideal organic assemblies active for nonlinear optics such as second harmonic generation (SHG). Extensive surveys have been made in evaluating the nonlinearities so as to find ideal structures consisting of molecules with large nonlinear susceptibilities. The difficulty in evaluating the molecular hyperpolarizability β using the LB technique arises from the fact that the monolayers cannot be perfectly formed. In consequence, a certain molecular arrangement has to be assumed, such as a unique tilt angle and a uniform distribution of the azimuth angle for the molecular long axis.[1,2]

The evaluation not only of the molecular hyperpolarizability but also the second order nonlinear susceptibility $\chi^{(2)}$ possesses several problems. Most experiments show that the intensity of second harmonic (SH) light does not obey the square law of the number of layers; this is in conflict with theoretical expectations,[3-6] even though results confirming the square law have been obtained recently.[7-9] The imperfection in the monolayers may be one reason for the contradiction. The imperfection arises from several causes; it is well known that the use of cadmium

(II) improves film quality. Moreover, a LB film of dye molecules gives maximum SHG efficiency at a certain mixing ratio with fatty acid molecules,[10,11] which may originate from the formation of H-aggregates at high dye concentrations.[12] Some practical problems also exist in detecting SHG. For instance, an interference of SH lights from front and rear monolayer surfaces of a substrate should be taken into account. The interference fringes of SHG have been pointed out by Ledoux *et al.*[6] as dephasing between SH lights generated at the two surfaces caused by dispersion of the refractive index of the substrate as previously demonstrated for third harmonic generation from LB films.[13] Therefore, the SHG experiments performed with samples having monolayers on both surfaces at a fixed angle of incidence are meaningless from the viewpoint of determining absolute values of $\chi^{(2)}$ or β.

In this paper, various optical geometries are examined for the determination of the ratios of each component of $\chi^{(2)}$; *i.e.*, the directions of the incident light and of the signal detection relative to the substrate surface with a monolayer. It is shown that s-polarized-light excitation onto the monolayer from the air side (front-surface geometry) and from behind through the glass substrate (rear-surface geometry), gives rise to great differences in SHG, while the difference is negligible for p-polarized-light excitation.

2. EXPERIMENTS

2.1 Sample preparation

The sample used was a mixture of hemicyanine dye,

$$C_{20}H_{41}\ {}^{+}N(C_5H_4)(CH)_2(C_6H_4)N(CH_3)_2,$$

and arachidic acid,

$$C_{19}H_{39}COOH,$$

at a volume ratio of 1:2 (HEMI/AA); this ratio is close to the one showing optimum SHG efficiency.[11] It was dissolved in a 1 mmol/l solution of spectrum-class chloroform, the solution being spread on aqueous subphases and deposited onto glass substrates treated hydrophilically. Deposition was carried out at a surface pressure of 35 mN/m with the lifting speed of 6.2 mm/min in the aqueous subphase (pH = 5.6) with 0.7 mmol/l cadmium(II) chloride at 21°C.

The sample mainly used was a monolayer of (HEMI/AA) on one substrate-surface, obtained by deposition onto two attached glass substrates. A substrate with a monolayer on both surfaces was also used for comparison.

2.2 SHG measurements

The experimental setup for SHG measurements is illustrated in Figure 1. A Q-switched Nd^{3+}:YAG laser (Quanta-Ray DCR-11, $\lambda = 1.064\ \mu m$; pulse duration

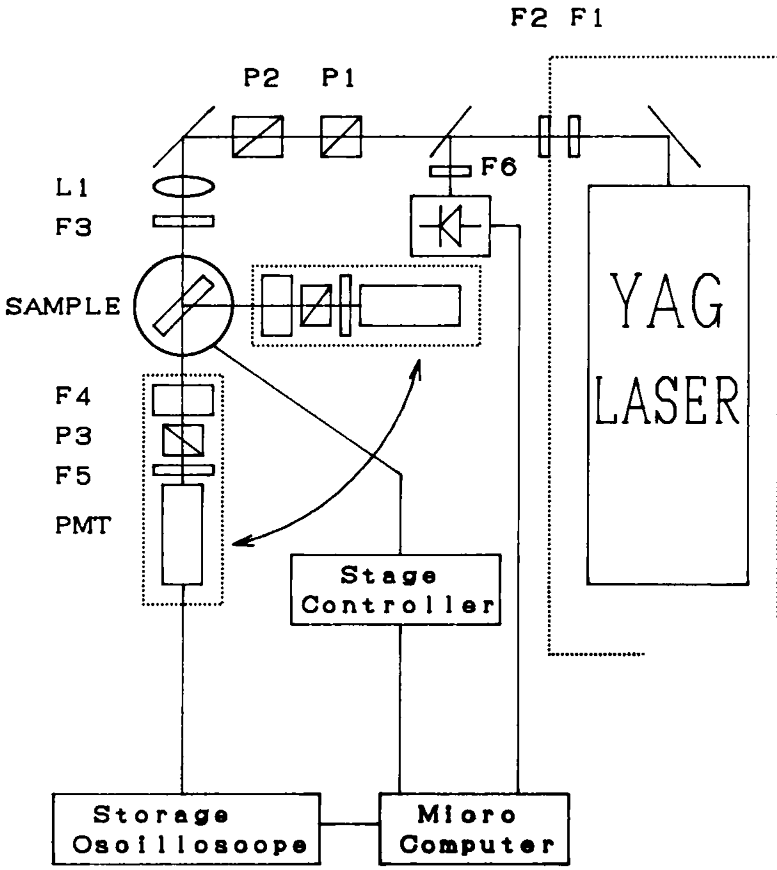

FIGURE 1 Experimental setup for SHG measurement; F1 and F6 (ND filter), F2 and F3 (IR pass filter), F4 [copper(II) sulfate filter], F5 (SH pass filter), P1 (λ/4 plate), P2 (polarizer), P3 (analyzer), L1 (lens).

10 ns; repetition rate 10 Hz) was used after decreasing the pulse energy down to less than 10 mJ by projecting the beam off a reflector and through an ND filter (FI). To prevent contamination from visible light emitted by the flashlamp, the YAG laser was placed in a dark box and the beam passed through a window of an interference filter (F2). The polarization of the fundamental beam was chosen using a λ/4 wave plate (P1) and a linear polarizer (P2). To eliminate SH light from the optical components such as the lens, a visible cut filter (F3) was inserted just before the sample cell. The optical components for SH light detection, a copper(II) sulfate solution filter (F4) and an interference filter (F5) to pass only the SH light, a linear polarizer and a photomultiplier tube (PMT, Hamamatsu R446), were located on a goniometer-arm, so that the detection was made from either the reflected or the transmitted direction. The signal from the PMT together with the signal of the fundamental beam from a photodiode were sent to a storage oscilloscope (Philips 3320). The stored and accumulated signals were processed by a microcomputer (NEC PC 9801 VM2). The computer was also used for controlling the rotation of a sample stage with a stepping motor.

3. EXPERIMENTAL RESULTS

Figure 2 shows the SH intensity as a function of the incident angle. P-polarized SH light was detected using p- and s-polarized fundamental beams (p→p and s→p) along the transmitted direction ($I_T^{p\to p}$ and $I_T^{s\to p}$). The sample used was monolayers of (HEMI/AA) on both surfaces and a single surface of the substrate. Figures 2(a), (b) and (c) are $I_T^{p\to p}$ from both surfaces, $I_T^{s\to p}$ from both surfaces and $I_T^{p\to p}$ from a single surface, respectively. The profile of $I_T^{s\to p}$ from a single surface is essentially the same as that in Figure 2 (c). Interference fringes due to SH light from both surfaces are clearly observed in Figure 2 (a) and (b). It should be noted that the fringe minima increase with an incident angle for $I_T^{s\to p}$ while they stay almost zero for $I_T^{p\to p}$. The sample with a monolayer on a single surface shows, on the contrary, a smooth change in SH intensity without a fringe structure as shown in Figure 2 (c), although Ledoux *et al.*[6] reported a fringe pattern due to multiple reflection inside the substrate even in a LB film on one side.

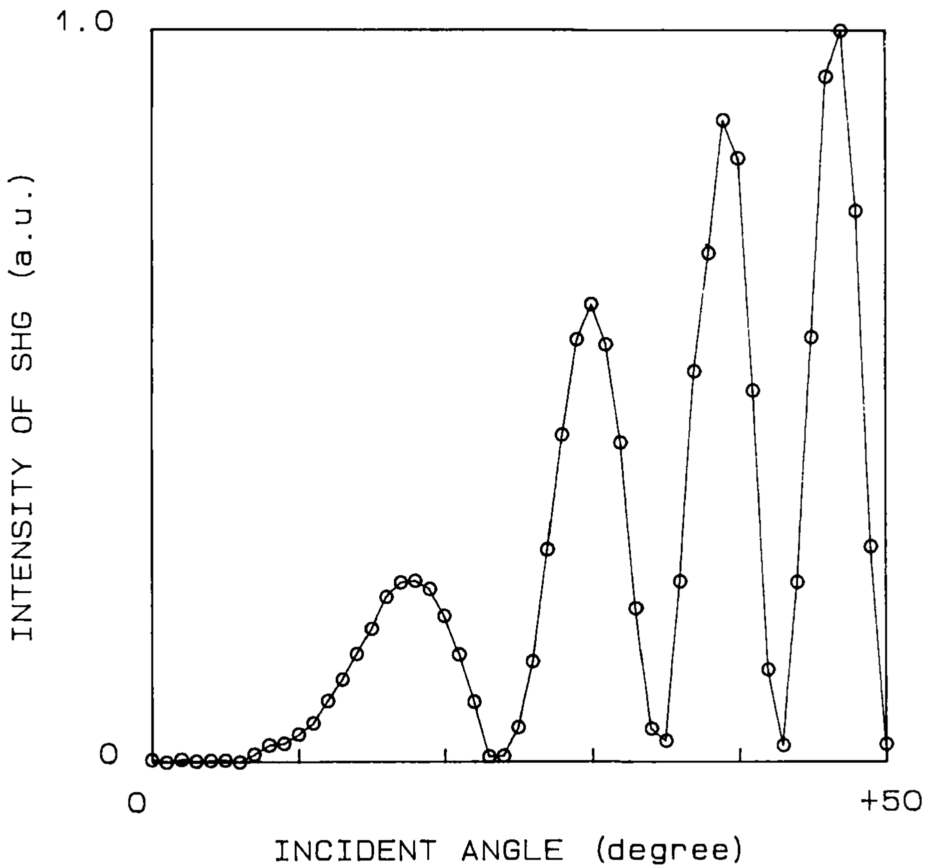

(a)

FIGURE 2 Incident angle dependence of the SH intensities; (a) $I_T^{p\to p}$ from monolayers on both glass surfaces, (b) $I_T^{s\to p}$ from monolayers on both surfaces and (c) $I_T^{p\to p}$ from a monolayer on a single surface.

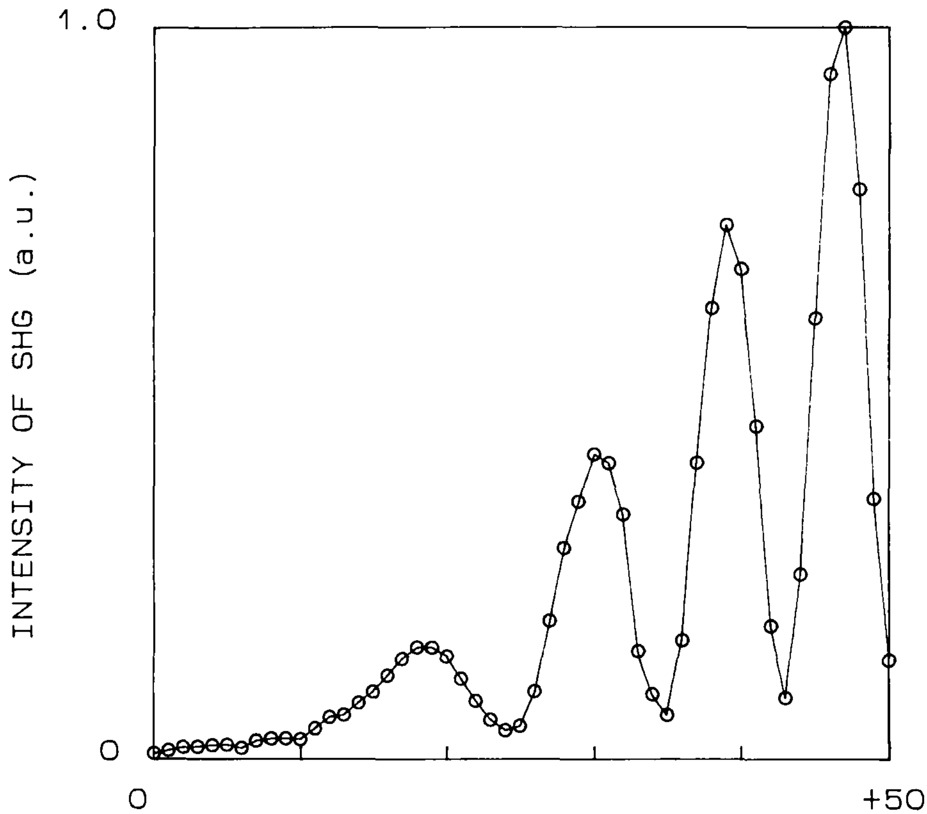

(b)

FIGURE 2 (*continued*)

In order to see the direction of SH light emitted, SH light intensities along the transmitted and the reflected directions, I_T and I_R, were measured as the goniometer arm, where PMT is located, was slightly rotated. Figure 3 shows the results for $I_T^{p \to p}$ and $I_T^{s \to p}$, when the incident angle was fixed at 45°. At an angle of 0.5° out of true from the transmitted direction, I_T decreases to about 50% of the maximum. Thus, the direction in which SH light is emitted is quite restricted. The same behavior was also observed for SH light observed from the reflected direction, although the damping at off angles was less conspicuous because of the weak signal comparable with the noise level. The above results seriously influence the analysis of Figure 2, since the SH beam laterally shifts due to a refraction at interfaces of the substrate glass and air.

All the experiments described above were performed using samples with a monolayer on front surface or both surfaces. SHG measurements were also made for a sample with a monolayer on the rear surface of a substrate at 45° incidence. The optical geometries and the results are shown in Figures 4 (a) and (b), where

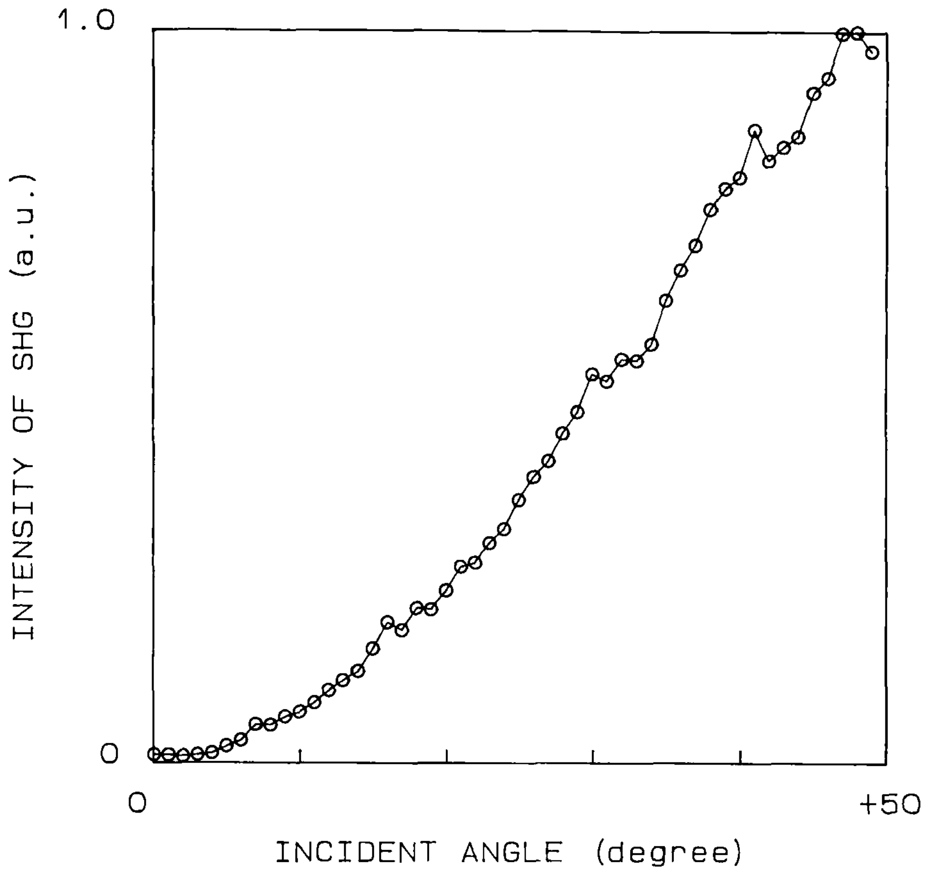

(c)

FIGURE 2 (*continued*)

the SH intensities are the ones normalized by $I_{Tf}^{p\to p}$. The subscript f stands for front. Similarly, the subscript r in Figure 4 stands for rear. The most remarkable feature is that the SH intensity by s-polarized light shows a difference between the two geometries of a factor of two or three as expected from Figure 2 (b). On the other hand, p-polarized light gives almost the same SHG in both optical geometries. These features are observed in both transmission and reflection geometries. The qualitative results for the front-surface geometry, $I_{Tf}^{p\to p} \gg I_{Tf}^{s\to p} \sim I_{Rf}^{p\to p} \sim I_{Rf}^{s\to p}$, agree with the ones by Neal *et al.*[10] and by Girling *et al.*[11]

SHG measurements were also made using a rectangular prism with a monolayer on the largest plane. The geometry and the results are shown in Figures 4(c) and (d), where SH intensities in various geometries are the ones normalized by $I_{Rf}^{p\to p}$. The actual SH intensities, $I_{Rf}^{p\to p}$, of the prism sample and of the glass-plate sample are more or less the same. Even the transmitted SH light was observed at almost the same ratio as that in the glass-plate sample. In the geometry of total internal reflection, the ratio $I_{Rr}^{p\to p}/I_{Rr}^{s\to p}$ was almost the same as that in Fresnel reflection, $I_{Rf}^{p\to p}/I_{Rf}^{s\to p}$.

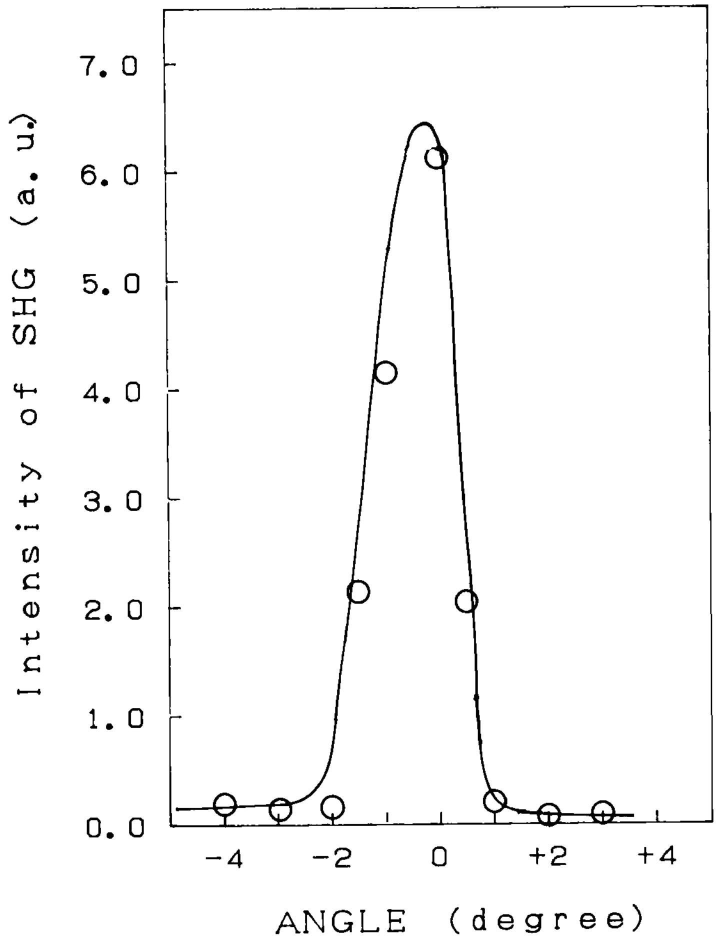

FIGURE 3 SH intensity in the transmission geometry as a function of rotating angle of a photomultiplier tube.

4. DISCUSSIONS

The results on the basis of a simplified model, neglecting Fresnel factors, are analyzed first to show how the results for the rear-surface geometry are anomalous. It is assumed that the deposited molecules have their optical axis normal to the surface, in other words, the tilt of the molecular long axis from the surface normal is randomly distributed over the whole azimuth angle. Therefore, the point symmetry of the LB film is $C_{\infty v}$ where the symmetry axis is taken as z. The nonlinear susceptibility tensor in this symmetry is given by

$$\chi^{(2)} = \begin{bmatrix} 0 & 0 & 0 & 0 & \chi_{xzx} & 0 \\ 0 & 0 & 0 & \chi_{yzy} & 0 & 0 \\ \chi_{zxx} & \chi_{zyy} & \chi_{zzz} & 0 & 0 & 0 \end{bmatrix}, \qquad (1)$$

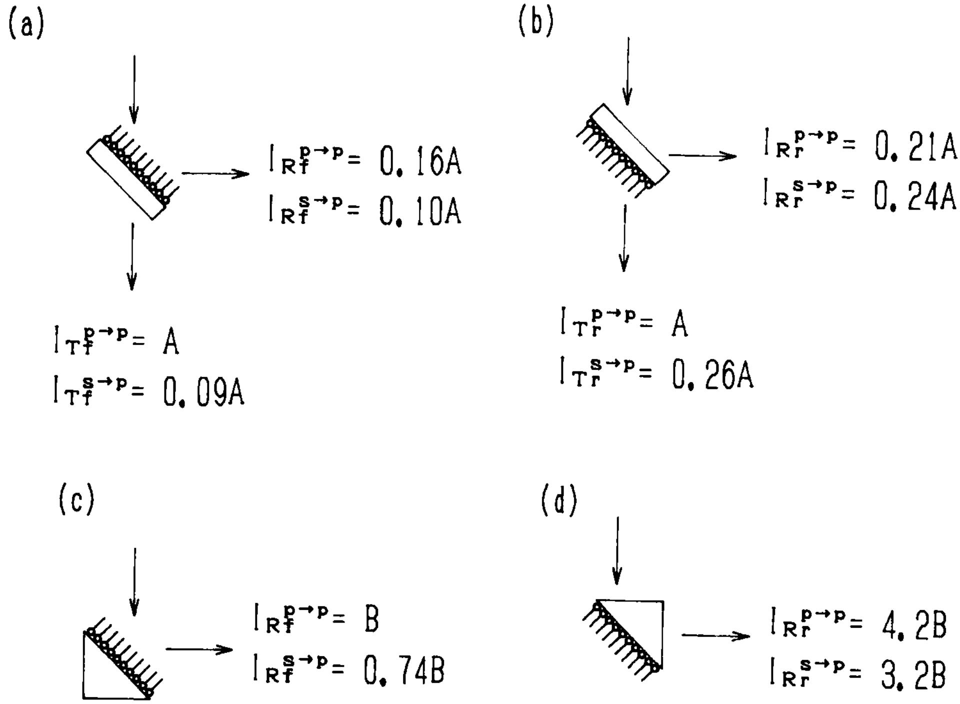

FIGURE 4 Various optical geometries for SHG measurements and normalized SH intensities in respective geometries; (a) front-surface geometry, (b) rear-surface geometry, (c) Fresnel reflection in a prism sample and (d) total internal reflection in a prism sample.

where $\chi_{xzx} = \chi_{yzy}$ and $\chi_{zxx} = \chi_{zyy}$. By assuming Kleinman's condition (although the condition may not valid because of the absorption band of hemicyanine dye), the number of independent components is further reduced to two; χ_{zzz} and $\chi_{xzx} = \chi_{yzy} = \chi_{zxx} = \chi_{zyy}$.

The second order nonlinear polarization is given by

$$P_i(2\omega) = \chi_{ijk}{}^{(2)}E_j(\omega)E_k(\omega). \tag{2}$$

Since the electric field vectors of p- and s-polarized incident light, $\boldsymbol{E}^p(\omega)$ and $\boldsymbol{E}^s(\omega)$, are given by

$$\boldsymbol{E}^p(\omega) = (-E_\omega \cos\theta,\ 0,\ E_\omega \sin\theta), \tag{3}$$

$$\boldsymbol{E}^s(\omega) = (0, E_\omega, 0) \tag{4}$$

in the optical geometry depicted in Figure 5, the values of the $\boldsymbol{P}(2\omega)$ are given by

$$\boldsymbol{P}^p(2\omega) = (-2\chi_{xzx}\sin\theta\cos\theta,\ 0,\ \chi_{zxx}\cos^2\theta + \chi_{zzz}\sin^2\theta)E_\omega{}^2, \tag{5}$$

$$\boldsymbol{P}^s(2\omega) = (0, 0, \chi_{zyy})E_\omega{}^2. \tag{6}$$

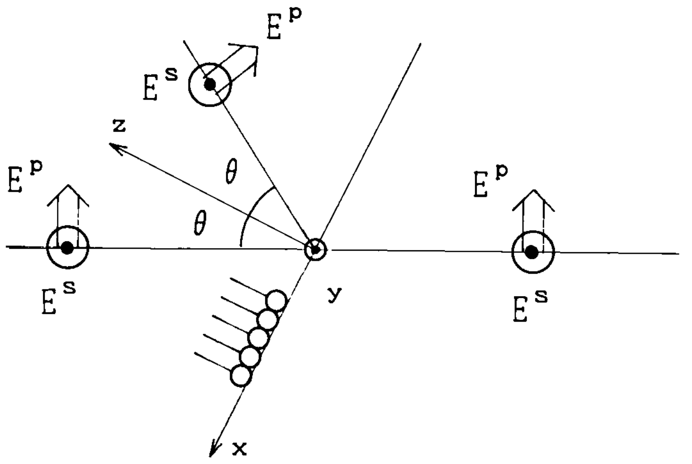

FIGURE 5 Optical geometry and coordinate system.

for p- and s-polarized incident light, respectively. Therefore, under Kleinman's condition, p-polarized SH intensities by p- and s-incidence (p → p and s → p) are expressed by

$$I_T^{p\to p} = (3\chi_{zxx} \sin\theta \cos^2\theta + \chi_{zzz} \sin^3\theta)^2 E_\omega^4, \tag{7}$$

$$I_T^{s\to p} = (\chi_{zxx} \sin\theta)^2 E_\omega^4, \tag{8}$$

for the transmission geometry, and

$$I_R^{p\to p} = (\chi_{zxx} \sin\theta \cos^2\theta - \chi_{zzz}\sin^3\theta)^2 E_\omega^4, \tag{9}$$

$$I_R^{s\to p} = (\chi_{zxx} \sin\theta)^2 E_\omega^4, \tag{10}$$

for the reflection geometry. It is easily shown that there is no s-polarized SH light, and this was actually the case in the present experiment.

Using Equations 7–10 and $\theta = 45°$,

$$\frac{I_T^{p\to p}}{I_T^{s\to p}} = \frac{1}{4}\left(3 + \frac{\chi_{zzz}}{\chi_{zxx}}\right)^2, \tag{11}$$

$$\frac{I_R^{p\to p}}{I_R^{s\to p}} = \frac{1}{4}\left(1 - \frac{\chi_{zzz}}{\chi_{zxx}}\right)^2, \tag{12}$$

$$\frac{I_T^{p\to p}}{I_R^{p\to p}} = \left(\frac{3 + \chi_{zzz}/\chi_{zxx}}{1 - \chi_{zzz}/\chi_{zxx}}\right)^2 \tag{13}$$

Substituting the experimental results for the front-surface geometry in Figure 4 into Equations 11, 12 and 13, values of χ_{zzz}/χ_{zxx} of 3.7, 3.5 and 3.6, respectively are obtained. The good agreement between these values deduced from different sets of experimental results supports the theoretical analysis made.

As for the experiments performed in the rear-surface geometry, it is clear that the above equations for the analysis are not adequate. Values of χ_{zzz}/χ_{zxx} of 0.63, 2.9 and 4.4, would be obtained if Equations 11, 12 and 13, respectively, were used.

It should be noted that the results for the transmitted s→p configuration in Figures 4(a) and (b) are consistent with the fringe pattern in Figure 2(b) where the fringe minima do not decrease to zero. The interference between the two waves, $E\sin\omega t$ and $\alpha E\sin(\omega t + \delta)$, gives rise to an intensity proportional to $(1 + \alpha^2) + 2\alpha \cos \delta$. Therefore, the ratio of fringe maxima and minima is given by $\{(1 + \alpha)/(1 - \alpha)\}^2$. In Figures 4(a) and (b), $\alpha^2 = I_{Tr}^{s\to p}/I_{Tf}^{s\to p}$ is about 3, resulting in $\{(1 + \alpha)/(1 - \alpha)\}^2 \approx 14$, which is comparable to the ratio of fringe maxima and minima, about 10, in Figure 2(b). Thus, the great differences in SHGs given by front and rear excitation in s→p configuration, $I_f^{s\to p}$ and $I_r^{s\to p}$, are consistently observed in two different samples which have two monolayers on both sides (Figure 2(b)) and a single monolayer (Figures 4 (a) and (b)).

It is impossible to attribute the great difference between $I_{Tr}^{s\to p}$ and $I_{Tf}^{s\to p}$ to the contribution from Fresnel reflection in linear optics, since the reflectance is at most 10% in the present experimental set up. According to the theory of Dick *et al.*,[14] the SHG signal is enormously enhanced as total internal reflection occurs. However, there exist two difficulties in considering this effect as the main cause of $I_{Tr}^{s\to p} > I_{Tf}^{s\to p}$. Contrary to the s→p configuration, $I_f \approx I_r$ in the p→p configuration. Namely, the total internal reflection does not influence the p-polarized light excitation. Moreover, the enhancement is just three or four times both for s- and p-excitations as shown in Figure 4(c) and (d), although theory predicts an increase of about two orders of magnitude. For complete understanding, the simulation should be made of both s→p and p→p configurations using the theory of Dick *et al.*[14] as Guyot-Sionnest *et al.*[15] have done for the s→p configuration. This work is in progress and will be reported elsewhere.

References

1. T. F. Heinz, H. W. K. Tom and Y. R. Shen: *Phys. Rev.* **A28**, 1883 (1983).
2. G. Marowsky, A. Gierulski, R. Steinhoff, D. Dorsch, R. Eidenschnik and B. Rieger: *J. Opt. Soc. Am.* **B4**, 956 (1987).
3. I. R. Girling, P. V. Kolinsky, N. A. Cade, J. D. Earls and I. R. Peterson: *Opt. Commun.* **55**, 289 (1985).
4. I. R. Girling, N. A. Cade, P. V. Kolinsky, J. D. Earls, G. H. Cross and I. R. Peterson: *Thin Solid Films* **132**, 101 (1985).
5. L. M. Hayden, S. T. Kowel and M. P. Srinivasan: *Optic Commun.* **61**, 351 (1987).
6. I. Ledoux, D. Josse, P. Vidakovic, J. Zyss, R. A. Hann, P. F. Gordon, B. D. Bothwell, S. K. Gupta, S. Allen, P. Rabin, E. Chastaing and J. C. Dubois: *Europhys. Lett.* **3**, 803 (1987).

7. R. Popovitz-Biro, K. Hill, E. M. Landau, M. Lahav, L. Leiserowitz and J. Sagiv: *J. Am. Chem. Soc.* **110**, 2672 (1988).
8. G. Gecher, B. Tieke, C. Bosshard and P. Gunter: *J. Chem. Soc. Chem. Commun.* 933 (1988).
9. L. M. Hayden, B. L. Anderson, J. Y. S. Lam, B. G. Higgins, P. Stroeve and S. T. Kowel: *Thin Solid Films* **160**, 379 (1988).
10. D. B. Neal, M. C. Petty, G. G. Roberts, M. M. Ahmad, W. J. Feast, I. R. Girling, N. A. Cade, P. V. Kolinsky and I. R. Peterson: *Proc. 6th IEEE Int. Symp. on Applied Ferroelectrics* 89, (1986).
11. I. R. Girling, N. A. Cade, P. V. Kolinsky, R. J. Jones, I. R. Peterson, M. M. Ahmad, D. B. Neal, M. C. Petty, G. G. Roberts and W. J. Feast: *J. Opt. Soc. Am.* **B4**, 950 (1987).
12. J. S. Schildkraut, T. L. Penner, C. S. Willand and A. Ulman: *Opt. Lett.* **13**, 134 (1988).
13. F. Kajzar, J. Messier, J. Zyss and I. Ledoux: *Opt. Commun.* **45**, 133 (1983).
14. B. Dick, A. Gierulski, G. Marowsky and A. A. Reider: *Appl. Phys.* **B38**, 107 (1985).
15. P. Guyot-Sionnest, Y. R. Shen and T. F. Heinz: Appl. Phys. **B42**, 237 (1987).